Performance Enhancement of Precoded Point-to-Point Massive MIMO Systems Using Uniform and Non-uniform Quantized ADC/DACs

Girish Kumar N G[1,*] and M N Sree Ranga Raju[2]

[1]Department of Telecommunication Engineering, Bangalore Institute of Technology, Bangalore, India
[2]Department of Electronics and Communication Engineering, Bangalore Institute of Technology, Bangalore, India
Email: girishkumarng@bit-bangalore.edu.in (G.K.N.G.)
[*]Corresponding author
Manuscript received April 13, 2023; revised May 30, 2023; accepted July 10, 2023; published January 8, 2024

***Abstract*—This paper investigates the spectral and energy efficiency of a Precoded point-to-point massive MIMO system with low-resolution Analog to Digital Converters (ADCs) and Digital to Analog Converters (DACs), using both uniform and non-uniform quantization while considering the quantization noise. The authors propose an iterative alternating minimization algorithm to obtain the optimal hybrid precoder matrix and explore the trade-off between spectral and energy efficiency. The proposed system considers a single-user point-to-point massive Multiple Input and Multiple Output (MIMO) system with a base station and receiver equipped with low-resolution DACs and ADCs, respectively, and a narrow-band Rayleigh-fading channel. The simulation results show that the proposed Hybrid Precoding (HP) algorithm improves the spectral and energy efficiency of the massive MIMO system compared to a fully digital precoded system, with both Uniform and Non-Uniform Quantization. Transmit precoding is used to improve the downlink performance and simplify the receiver design in massive MIMO systems. However, this study shows that HP with low-resolution ADCs/DACs can achieve similar or better performance than Fully Digital Precoding (FDP), with significant reductions in hardware complexity and power consumption. The results suggest that HP can be a promising solution for future wireless communication systems. Future work could explore other channel models, different quantization schemes, and multi-user scenarios to further enhance the performance of HP in massive MIMO systems.**

***Keywords*—Massive Multiple Input and Multiple Output (MIMO) systems, hybrid precoding uniform quantization, non-uniform quantization, spectral efficiency, energy efficiency**

I. Introduction

Massive Multiple Input and Multiple Output (MIMO) is a key technology for 5G wireless communication systems, which enables high-capacity and high-throughput wireless communications. One of the major challenges in implementing massive MIMO systems is the need for efficient signal processing methods, especially in the design of Hybrid Precoding (HP) algorithms. Precoding is a technique used in massive MIMO systems to reduce the decoding complexity at the receiver and improve downlink performance. However, the use of high-resolution Analog to Digital Converters (ADCs) and Digital to Analog Converters (DACs) in precoding leads to high power consumption and increased hardware complexity. Therefore, low-resolution ADC/DAC quantization is an attractive solution for realizing cost-effective and energy-efficient massive MIMO systems.

In recent years, there has been significant research interest in the design of efficient precoding algorithms for massive MIMO systems using both Uniform Quantized (UQ) and Non-Uniform Quantized (NUQ) ADC/DACs. Chataut and Akl [1] provided an overview of the current state-of-the-art in massive MIMO systems for 5G and beyond networks, highlighting recent trends, challenges, and future research directions. The authors also discuss the potential of low-cost analog and Radio Frequency (RF) components for achieving high data rates in massive MIMO systems. Hong *et al.* [2] discussed the role of millimeter-wave (mmWave) technologies in 5G and 6G wireless communications, exploring the challenges and opportunities of mmWave MIMO systems and their potential to address the capacity demands of future wireless networks.

To develop efficient beamforming algorithms for massive MIMO systems, Zhang *et al*. [3] proposed a holistic view of hybrid beamforming for 5G and beyond millimeter-wave systems, which considers the key challenges and design issues. To minimize energy consumption while maintaining high spectral efficiency, Hei *et al*. [4] proposed an algorithm for designing efficient HP matrices for mmWave MIMO systems with phase modulation arrays. Chen *et al.* [5] proposed a low-complexity hybrid analog and digital precoding algorithm for mmWave MIMO systems that achieves near-optimal performance with reduced computational complexity.

Several research studies have focused on the design of HP algorithms for mmWave massive MIMO systems. Ding *et al*. [6] proposed an HP algorithm for mmWave massive MIMO systems with different antenna arrays, improving the overall system performance by reducing the number of RF chains required. Pavia *et al*. [7] presented low-complexity HP designs for multiuser mmWave/THz ultra-massive MIMO systems, which reduce the hardware complexity and energy consumption of the system. Lu *et al.* [8] proposed a quantized HP design for millimeter-wave large-scale MIMO systems, which uses low-resolution ADCs and DACs to reduce power consumption and hardware complexity. Zhang *et al*. [9] compared the performance of hybrid and full-digital beamforming in mmWave massive MIMO systems, taking into account low-resolution ADCs. Dai *et al*. [10] investigated the achievable rates for full-duplex massive MIMO systems with low-resolution ADCs/DACs. The authors propose an HP algorithm that achieves near-optimal performance with reduced complexity.

Ren *et al*. [11] proposed an HP design algorithm for energy-efficient millimeter-wave massive MIMO systems. In this paper, the proposed algorithm outperforms other methods in terms of energy efficiency, especially on large-scale

DOI: 10.7763/IJCTE.2024.V16.1348

MIMO systems, and requires less hardware complexity. Li *et al*. [12] proposed a novel HP algorithm for millimeter-wave MIMO systems for both perfect and imperfect Channel State Information (CSI) scenarios, achieving near-optimal performance and being less sensitive to imperfect CSI.

In our proposed paper, we focus on the performance enhancement of Precoded point-to-point massive MIMO systems using both uniform and non-uniform quantized ADC/DACs. Specifically, we propose an iterative alternating minimization-based HP algorithm to optimize the hybrid precoder matrix for efficient signal processing in massive MIMO systems.

Our main contributions are as follows: Firstly, we use the Bussgang theorem and an additive quantization noise model to derive an expression of spectral efficiency for massive MIMO systems with low-resolution ADCs/DACs at the receiver/transmitter, respectively. Secondly, we analyze the impact of the resolution of ADCs/DACs on the performance of MIMO systems using both UQ and NUQ techniques, and we derive a unique algorithm for NUQ. Thirdly, we use an alternating minimization scheme to find the optimal precoder matrix. Finally, we investigate the trade-off between spectral and energy efficiency using different precoding schemes based on UQ and NUQ by varying the resolution of ADC/DACs, and we aim to determine better efficient precoding strategies. The obtained solutions achieve performance close to precoding schemes that are based on full-resolution UQ and NUQ DACs and ADCs.

The nomenclature of the symbols is listed in Table 1.

Table 1. Nomenclature

Abbreviation	Full name
SE	Spectral Efficiency(b/S/Hz)
N_t	Number of Transmitter Antennas
N_r	Number of Receiver Antennas
${N_t}^{RF}$	Number of RF chains at Base Station
${N_r}^{RF}$	Number of RF chains at Receiver
N_S	Number of Data Streams
D_{BB}	Digital Precoder Matrix
A_{RF}	Analog Precoder Matrix
P_t	Transmitted Power
$Q(.)$	Quantization Process
EE	Energy Efficiency (bits/Sec/Hz/Watts)
ζ	Distortion Factor of DAC
ρ	Distortion Induced by ADC
b	ADC Resolution
q	DAC Resolution
NUQ	Non Uniform Quantization
UQ	Uniform Quantization
CSI	Channel State Information

II. Literature Survey

In this literature survey, we offer an extensive review of recent research contributions in the fields of hybrid precoding, millimeter Wave (mmWave) channels, massive MIMO systems, and low-resolution ADCs and DACs. The main objective of this survey is to scrutinize the methodologies employed in these studies, evaluate their strengths and weaknesses, and investigate the use of uniform and non-uniform quantization techniques. A noteworthy observation from this survey indicates that none of the reviewed papers explored the application of non-uniform quantization for low-resolution ADCs/DACs, which could potentially lead to enhanced performance in these systems.

Shaban *et al*. [13] contributed valuable insights into statistically-aided codebook-based HP methods for mmWave channels with a partially connected structure. Huang *et al.* [14] proposed a Discrete Fourier Transform (DFT) codebook-based HP scheme for multiuser mmWave massive MIMO systems. Almradi *et al*. [15] introduced an HP method for massive MIMO systems with low-rank channels using a two-stage user scheduling approach. Zhang *et al.* [16] compared hybrid and full-digital beamforming in mmWave massive MIMO systems, taking into account low-resolution ADCs. Liu *et al.* [17] contributed to the field of achievable rates for full-duplex massive MIMO systems with low-resolution ADCs/DACs by further enhancing the understanding of system performance. In comparison to [17], our study incorporates the analysis of quantization error, loop interference, and inter-user interference to provide a more comprehensive evaluation. Moreover, we emphasize the effectiveness of power scaling and increased ADC/DAC resolution in mitigating interference and noise. These findings underscore the superiority of our approach in improving the achievable rates and validate the significance of adopting low-resolution ADCs/DACs in FD massive MIMO systems. Dai *et al*. [18] investigated the achievable rates for full-duplex massive MIMO systems with low-resolution ADCs/DACs. Ding *et al*. [19] analyzed the spectral and energy efficiency of HP for mmWave massive MIMO systems with low-resolution ADCs/DACs. Xiong [20] evaluated the achievable rates for massive MIMO relaying systems with variable-bit ADCs/DACs.

Ding *et al*. [21] performed a performance analysis of full-duplex massive MIMO systems with low-resolution ADCs/DACs over Rician fading channels, emphasizing the effect of channel conditions on system performance. Xu and Ren *et al*. [22] examined the security of massive MIMO downlink systems with low-resolution ADCs/DACs in the presence of active eavesdropping, underscoring the need to address potential security vulnerabilities. Xiong *et al.* [23] assessed the performance of massive MIMO relay systems with variable-resolution ADCs/DACs over spatially correlated channels, illustrating the impact of variable-resolution quantization on system performance.

Wang *et al*. [24] concentrated on the joint optimization of spectral efficiency and energy efficiency with low-precision ADCs in cell-free massive MIMO systems, shedding light on the trade-offs between these two performance metrics. Zhang *et al.* [25] investigated secure transmission in cell-free massive MIMO systems with RF impairments and low-resolution ADCs/DACs, highlighting the challenges posed by hardware imperfections. Li *et al*. [26] carried out a downlink analysis for Device-to-Device (D2D) underlaid multigroup multicast cell-free massive MIMO systems with low-resolution ADCs/DACs, exploring the interactions between D2D and multigroup multicast communications.

Zhang *et al.* [27] analyzed indoor Terahertz (THz) communication systems with finite-bit DACs and ADCs, providing a perspective on the unique challenges faced in THz communication environments. Balti and Evans [28] examined full-duplex massive MIMO cellular networks with low-resolution ADC/DAC, focusing on the performance analysis of full-duplex systems in cellular network settings. Zhou *et al*. [29] studied multigroup multicast downlink cell-

free massive MIMO systems with multi-antenna users and low-resolution ADCs/DACs, revealing the impact of multi-antenna users on system performance.

Kim *et al*. [30] assessed cell-free mmWave massive MIMO systems with low-capacity front haul links and low-resolution ADC/DACs, delving into the implications of front haul link capacity constraints. Zhang *et al*. [31] explored massive MIMO systems with low-resolution ADCs, focusing on achievable rates and allocation of quantization bits, offering insights into bit allocation strategies for low-resolution systems.

The use of one-bit ADCs in massive MIMO systems presents significant challenges in achieving reliable detection and decoding. Park and Lee *et al*. [32] propose a novel learning-based approach to address these challenges. By replacing the traditional channel estimation stage with a counting-based learning process, the proposed technique reduces the impact of quantization noise and improves detection accuracy. This work aligns with our research on HP in massive MIMO systems with low-resolution ADCs and DACs. By incorporating adaptive learning techniques, similar to those proposed in the referenced paper, we aim to enhance the performance of our HP scheme, optimize spectral and energy efficiency, and improve overall system performance.

Park and Lee *et al*. [32] addressed the challenge of high cost and power consumption associated with the increasing number of RF chains in massive MIMO systems. Specifically, they focus on the application of low-resolution Digital-to-Analog Converters (DACs) in multi-carrier systems, which have received limited attention thus far. Wen and Qian *et al*. [33] proposed a 1-bit downlink precoding algorithm for massive multi-user MIMO Orthogonal Frequency Division Multiplexing (OFDM) systems. The algorithm tackles the non-convex optimization problem with discrete output constraints and incorporates considerations for different path losses experienced by users. The proposed algorithm performs better than other nonlinear precoding methods in OFDM systems. This work aligns with our research on HP in massive MIMO systems, as both studies aim to optimize system performance and reduce power consumption by leveraging low-resolution DACs. By considering the insights from this paper, we can further enhance our HP scheme and its applicability in multi-carrier OFDM systems.

Despite the significant contributions provided by these works, the potential benefits of non-uniform quantization remain unexplored. Implementing non-uniform quantization could offer several advantages over the uniform quantization techniques discussed in the reviewed literature, including:

- Enhanced system performance due to improved quantization noise reduction.
- Increased spectral and energy efficiency resulting from better handling of the signal dynamic range.
- Potential reduction in hardware complexity and power consumption due to more efficient use of ADC/DAC resolution.

In conclusion, while the existing literature provides substantial insights into the design and performance analysis of full-duplex massive MIMO systems and related areas with low-resolution ADCs/DACs, there is a clear gap in the examination of non-uniform quantization. Future research should focus on exploring the benefits of non-uniform quantization in these systems, which could potentially lead to more efficient and higher-performing solutions for mmWave and massive MIMO applications.

Our research stands out from existing works as we address a critical gap in the literature by exploring the usage of non-uniform quantization in the context of low-resolution DAC and ADC-based hybrid precoding. By leveraging non-uniform quantization, we unlock the potential for improved performance, reduced hardware complexity, and enhanced energy efficiency in massive MIMO systems.

III. System Overview

In this section, we will provide an overview of the system considered in our work. Specifically, we have analyzed a single-user point-to-point massive MIMO system consisting of N_t transmitter antennas at the base station and a single receiver with N_r receiver antennas. Fig. 1 illustrates an FDP massive MIMO system, where each of the N_t transmitter antennas is connected to an individual RF chain and sends N_S streams of data symbols, represented by a vector S, through an array of N_t transmitter antennas. On the other hand, Fig. 2 shows an HP massive MIMO system, where each transmitter antenna is connected to a selected RF chain, and N_S streams of data symbols are sent through the array of N_t transmitter antennas to the N_r receiver antennas.

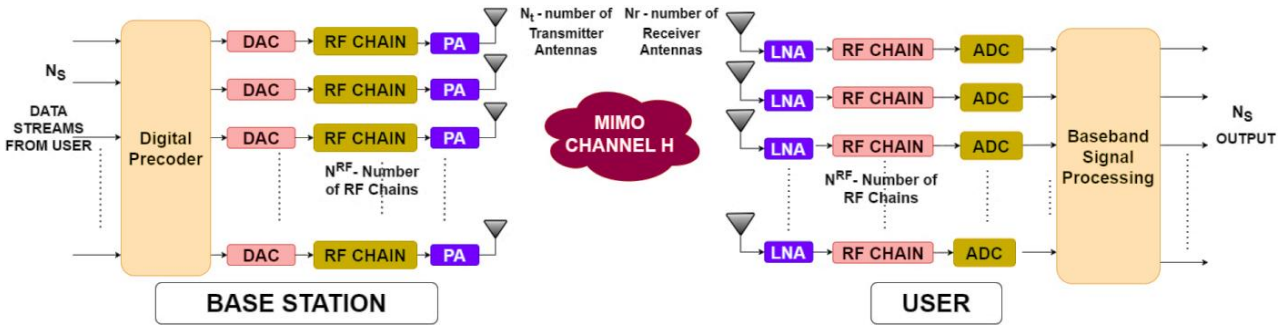

Fig. 1. Fully digital precoded massive MIMO system.

The user data is scrambled, encoded, and modulated. The modulated data is digitally precoded using a $N_t{}^{RF} \times N_S$ digital precoder, where N_{RF} is the number of RF chains and N_S is the number of streams. Each of the $N_t{}^{RF}$ streams is OFDM modulated. The OFDM modulated symbols are converted to the analog domain using NUQ low-resolution DAC. The IFFT output, which is a complex number, is split into Inphase and Quadrature (I/Q). Each I/Q is converted to

equivalent analog data and modulated using I/Q modulator. To maintain the desired amplitude of the symbols, a Variable Gain Amplifier (VGA) is used to boost the I/Q symbols prior to up-conversion. The upconverted signal is passed through a Bandpass Filter (BPF) to limit the spectrum to the desired band and then amplified using a Power Amplifier (PA). The output of the PA is phase-shifted using a phase shifter and analog precoded before being radiated into free space.

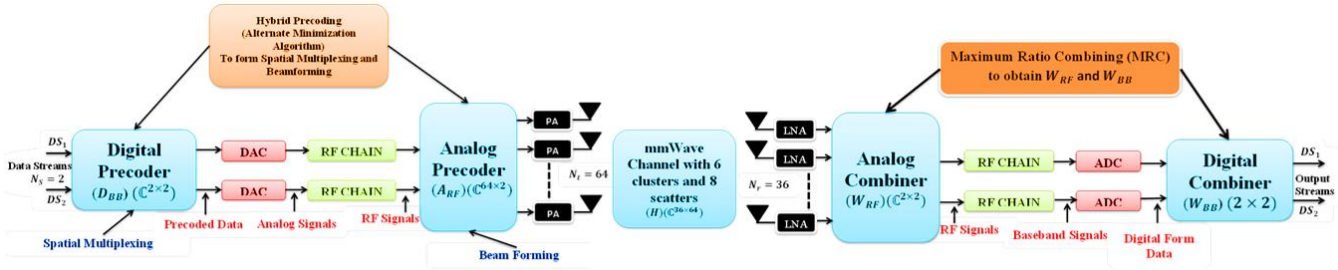

Fig. 2. Hybrid precoded massive MIMO system.

Each receiving antenna at the receiver passes the received input through a Low-Noise Amplifier (LNA) to boost the signal without adding noise, thereby improving the SNR. The output of each LNA is combined at the analog combiner stage, and the combined outputs are then passed through the bandpass filter of each RF chain before being down-converted and passed through I/Q demodulation. The resulting analog signal is then converted to digital using a low-resolution ADC. The digital I/Q is then OFDM demodulated (FFT), and the digital combiner, which is the inverse of the digital precoder, is applied to the output. The resulting signal is then constellation de-mapped and decoded, and the output of the decoder is descrambled to produce an estimated copy of the transmitted user data.

Transmitted symbols are assumed to be independent and Gaussian-distributed random variables with zero mean and unit variance [18]. The digital precoder produces a digital precoder matrix $D_{BB} \in \mathbb{C}^{{N_t}^{RF} \times N_S}$, and the precoded data is passed through a DAC before being processed by an analog precoder to generate an analog precoded matrix $A_{RF} \in \mathbb{C}^{N_t \times {N_t}^{RF}}$. At the output of the transmitter, the transmitted vector $x \in \mathbb{C}^{N_t \times 1}$ is obtained by combining the precoded data with the digital precoder matrix and the analog precoder matrix. At the output of the transmitter the transmitted vector $x \in \mathbb{C}^{N_t \times 1}$ is obtained by:

$$x = \sqrt{P_t} A_{RF} Q_D(D_{BB} S) \tag{1}$$

where $Q_D(.)$ represents the Quantizer function and P_t is the normalized transmitted power. The transmitted vector undergoes multipath fading due to channel imperfections. After multipath fading, assuming a narrow band fading channel and no intersymbol interference [18] the received vector $y \in \mathbb{C}^{N_t \times 1}$ is given as:

$$y = Hx + n \tag{2}$$

Here, $H \in \mathbb{C}^{N_r \times N_t}$ represents the channel matrix capturing a channel perturbation of a discrete-time mmWave narrow Band Channel in which there is no mutual coupling and correlation between transmitter and receiver antennas is been considered and $n \in \mathcal{CN}(0, I_{{N_t}^{RF}})$ is the additive white gaussian noise.

$$H = \sqrt{\frac{N_t N_r}{L}} \sum_{l=1}^{L} \alpha_l f_r(\varphi_l{}^r, \theta_l{}^r) f_t{}^H(\varphi_l{}^r, \theta_l{}^r) \tag{3}$$

where $f_r(\varphi_l{}^r, \theta_l{}^r)$ and $f_t(\varphi_l{}^r, \theta_l{}^r)$ are antenna array response vectors of receiver and transmitter respectively and α_l is the complex gain of path l.

Since the received values go through ADC, before getting processed in the baseband, the received vector $r \in \mathbb{C}^{N_r \times 1}$ after ADC quantization can be given as:

$$r = Q_A(y) = Q_A(Hx + n) \tag{4}$$

On the transmitter side, the symbols are converted to analog data by multiple DACs. After DAC processing desired signal components are obtained by using the Bussgang Theorem [18] (Bussgang Theorem states that the cross-correlation between any two Gaussian signals is the same before and after one of them has passed through a non-linear function) which is given by:

$$t = Q_D(D_{BB} S) = F D_{BB} S + g \tag{5}$$

where $D_{BB} = [D_1 + D_2 + D_3 + \cdots + D_{{N_t}^{RF}}]^T$ input signal of the quantizer and F is the DAC processing matrix which is given by $F = (1 - \zeta) I_{N_{RF}}$ where ζ is the distortion factor of DACs and the uncorrelated Quantization error $g \in \mathbb{C}^{{N_t}^{RF} \times 1}$. Therefore using Eqs. (1), (2), and (5) the signal after the DAC process is given by:

$$y = (1 - \zeta)\sqrt{P_t} H A_{RF} D_{BB} S + \sqrt{P_t} H A_{RF} g + n \tag{6}$$

At the receiver side, the signal detected is quantized by ADCs. Using the Additive Quantization Noise Model [18], the quantizer output is calculated by:

$$r = \mathrm{Q_A}(y) = (1 - \rho) y + e \tag{7}$$

where ρ is the distortion induced by ADC and 'e' is the distortion noise of order $N_r \times 1$. Substituting Eqs. (1), (2), and (6) into Eq. (7) we get,

$$\begin{aligned} \mathrm{r} &= (1 - \rho)(1 - \zeta)\sqrt{\mathrm{P_t}} H A_{RF} D_{BB} S \\ &+ (1 - \rho)\sqrt{P_t} H A_{RF} g + (1 - \rho) n + e \end{aligned} \tag{8}$$

From Eq. (8), it can be seen that the received vector is linearly dependent on the choice of precoding matrices $\mathrm{A_{RF}}$

and D_{BB}. The matrix A_{RF} is the $N_t \times N_t^{RF}$ dimension Analog precoding matrix, that captures the weights of phase shifters, and the matrix D_{BB} is the $N_t^{RF} \times N_S$ dimension digital precoding matrix that captures the weights of digital precoding.

IV. UQ and NUQ Process for Low-Resolution DAC/ADC

The quantization process involves converting inputs with continuous values into outputs with a finite number of discrete levels. Usually, UQ is employed, where partition cells have equal size and shape. However, UQ may not always be the best option for natural signals like speech signals, as infrequent large signals are given poor quality, and frequent small amplitude signals may suffer from noticeable truncation effects. A quantizer that uses wider partition cells at high amplitude levels and narrower partition cells at lower amplitude levels can offer better performance than UQ. NUQ with companding is a method that can significantly reduce distortion compared to UQ. The effectiveness of NUQ in low-resolution ADCs/DACs can depend on various factors, such as the specific application, the nature of the input signal, and the quantization scheme used. However, in general, NUQ has been shown to provide better performance compared to UQ in low-resolution ADCs. This is because NUQ can allocate more bits to the parts of the signal that are more perceptually important, allowing for a more accurate representation of those parts. In contrast, UQ allocates an equal number of bits to all parts of the signal, which can result in poorer performance for signals with a wide dynamic range or a non-uniform distribution of energy. Therefore, in the context of low-resolution ADCs/DACs, NUQ techniques may be more effective in enhancing the Spectral and Energy Efficiency Performance of Single User Point to Point Massive MIMO systems. However, the specific type of NUQ and other system parameters should be carefully considered and evaluated through simulation and analysis.

The equation for NUQ using low-resolution ADC and DAC depends on the specific quantization scheme used. However, in general, the NUQ process involves dividing the input signal into a set of quantization intervals, where each interval has a non-uniform width. The non-uniform widths of these intervals can be determined based on a variety of criteria, such as perceptual importance, signal statistics, or some other optimization criteria. The quantized output of a NUQ system can be expressed as $q(n) = Q(x(n))$. where $x(n)$ is the input signal, $q(n)$ is the quantized output, and $Q(.)$ represents the non-uniform quantization function that maps the input signal to the quantization intervals. The quantization function $Q(.)$ can be implemented using lookup tables, polynomial approximations, or other methods. The output of the quantization function is then rounded to the nearest digital code that can be represented by the low-resolution ADC/DAC.

Overall, the specific equation for NUQ using low-resolution ADC and DAC will depend on the specific quantization scheme used and other factors such as the input signal properties and the specific hardware implementation. In our proposed work NUQ is derived from a Uniform quantizer using a companding function φ that is non-decreasing and smooth, followed by quantization using a Uniform quantizer Q with K equal interval levels. The output samples are then expanded using the function φ^{-1}.

Eq. (9) represents the standard algorithm for UQ, while Eqs. (10) and (11) represent the standard algorithms for NUQ [23].

$$x_i{}^q = \left[\frac{x_i - x_{min}}{q}\right] \times q + x_{min} \tag{9}$$

The NUQ μ-law quantizer can be given by:

$$x_i{}^{\mathrm{q}} = exp\left(1 + ln(1+\mu)\left(\frac{|x_i|}{x_{max}}\right)\right) * sign(x_i)$$

$$x_i{}^{\mathrm{q}} = \frac{ln(1+\mu|x_i|)}{ln(1+\mu)} * sign(x_i) \tag{10}$$

The NUQ A-law quantizer can be given by:

$$x_i{}^{\mathrm{q}} = \frac{ln\left(1 + log\left(\frac{A|x_i|}{x_{max}}\right)\right.}{1 + logA} \tag{11}$$

One can observe that UQ relies on the minimum value of x, while NUQ depends on the maximum value of x. Moreover, the quantized value is affected exponentially and/or logarithmically by the unquantized value. Given this dependence on the precoded symbol, the goal is to find an appropriate NUQ that can minimize distortion. To this end, we have developed a customized NUQ equation that takes into account the aforementioned dependencies. The derived custom NUQ equation is provided below.

$$x_i{}^q = \left[\frac{x_i(2^q - 1)}{(2^q - 1)}\right] * sign(x_i) * \left[\frac{x_{max} - x_{min}}{2^q + 1}\right] \tag{12}$$

In the above equation, the operator $*$ is the round-off operator, x_{max}, x_{min} maximum and minimum value of user precoded symbols and $x_i{}^q$ stands for quantized data.

V. Precoder Design and Analysis of Spectral Efficiency and Energy Efficiency

In this section, we will explore the necessary expression for computing the Spectral Efficiency (SE) and Energy Efficiency (EE) of a Massive MIMO system that employs low-resolution quantized converters. Additionally, we will delve into the iterative alternating minimization algorithm that is commonly used for Hybrid Precoder Design. To begin, SE is a measure of the amount of data that can be transmitted over a given bandwidth in a communication system. In the case of Massive MIMO systems with low-resolution quantized converters, the SE can be expressed as the ratio of the achievable data rate to the total bandwidth. On the other hand, EE is a metric that indicates the amount of information that can be transmitted per unit of energy consumed. In this context, the EE can be defined as the ratio of the achievable data rate to the total power consumption.

To achieve high SE and EE in Massive MIMO systems with low-resolution quantized converters, the design of the Hybrid Precoder becomes critical. The Hybrid Precoder is responsible for mapping the digital signals onto the analog domain, which is then transmitted through the antennas. An iterative alternating minimization algorithm is commonly

used for the design of the Hybrid Precoder, which involves optimizing the analog and digital precoders iteratively. The algorithm aims to minimize the total Mean Squared Error (MSE) between the actual and the desired signal, while also taking into account the constraints imposed by the low-resolution quantized converters. This algorithm is effective in achieving high SE and EE in Massive MIMO systems with low-resolution quantized converters.

A. Analysis of Spectral Efficiency

The SE is logarithmically proportional to the Signal to Interference Noise Ratio (SINR) for a Massive MIMO system is formulated as [18]:

$$SE = log_2 \left| I_{N_r} + \frac{Signal\ Power}{Noise\ Power} \right| \tag{13}$$

$$SE = log_2 \left| I_{N_r} + \frac{R_{\hat{S}\hat{S}}}{R_{\hat{g}\hat{g}} + R_{\hat{n}\hat{n}} + R_{\hat{e}\hat{e}}} \right| \tag{14}$$

The desired signal power $R_{\hat{S}\hat{S}}$ which is a covariance matrix of the desired signal part of the received vector r is calculated by:

$$\begin{gathered} R_{\hat{S}\hat{S}} = \mathbb{E}\left[\hat{S}\hat{S}^H\right] \\ = \mathbb{E}\left[\begin{matrix} \left((1-\rho)(1-\zeta)\sqrt{P_t}HA_{RF}D_{BB}S\right) \\ \left((1-\rho)(1-\zeta)\sqrt{P_t}S^H {D_{BB}}^H {A_{RF}}^H H^H\right) \end{matrix}\right] \end{gathered} \tag{15}$$

$$\begin{gathered} R_{\hat{S}\hat{S}} = (1-\rho)^2(1-\zeta)^2 P_t HA_{RF} \\ D_{BB}\mathbb{E}[SS^H]{D_{BB}}^H {A_{RF}}^H H^H \end{gathered} \tag{16}$$

As transmitted N_S data symbol $S = [S_1 + S_2 + S_3 + \cdots + S_{N_s}]^T$ are considered to be independent and Gaussian Distributed variable with zero mean and unit Variance, Therefore their covariance will be:

$$\mathbb{E}[SS^H] = \frac{1}{N_S} \times I_{N_S} \tag{17}$$

Therefore, by substituting Eq. (16) to Eq. (15), Desired Signal Noise Power is given by:

$$\begin{gathered} R_{\hat{S}\hat{S}} = (1-\rho)^2(1-\zeta)^2 \\ \left(\frac{P_t}{N_S}\right) HA_{RF}D_{BB}{D_{BB}}^H {A_{RF}}^H H^H \end{gathered} \tag{18}$$

The DAC Distortion noise power $R_{\hat{g}\hat{g}}$ which is a covariance matrix of DAC-induced distortion g and is given by:

$$\begin{gathered} R_{\hat{g}\hat{g}} = \mathbb{E}[\hat{g}\hat{g}^H] = \mathbb{E}\left[\begin{matrix} \left((1-\rho)\sqrt{P_t}HA_{RF}g\right) \\ \left((1-\rho)\sqrt{P_t}g^H {A_{RF}}^H H^H\right) \end{matrix}\right] \\ = (1-\rho)^2 P_t HA_{RF}\mathbb{E}[gg^H]{A_{RF}}^H H^H \end{gathered} \tag{19}$$

$$\begin{gathered} \mathbb{E}[gg^H] = \zeta(1-\zeta)diag(R_{dd}), \\ R_{dd} = \mathbb{E}[dd^H],\ d = D_{BB}S \end{gathered} \tag{20}$$

$$\begin{gathered} \mathbb{E}[dd^H] = \mathbb{E}\left[D_{BB}SS^H {D_{BB}}^H\right] \\ = D_{BB}\mathbb{E}[SS^H]{D_{BB}}^H \end{gathered} \tag{21}$$

Therefore the DAC Distortion Noise Power is given by:

$$R_{\hat{g}\hat{g}} = k\zeta(1-\zeta)(1-\rho)^2 \frac{P_t}{N_S} HH^H \tag{22}$$

The White Gaussian Noise Power $R_{\hat{n}\hat{n}}$ is obtained by:

$$\begin{gathered} R_{\hat{n}\hat{n}} = \mathbb{E}[\hat{n}\hat{n}^H] = (1-\rho)^2\mathbb{E}[nn^H], \\ \mathbb{E}[nn^H] = I_{N_r} \end{gathered} \tag{23}$$

Therefore, from Eq. (6), e follows $n \in \mathrm{C\dot{N}}(0, \mathrm{R}_{\hat{e}\hat{e}})$

$$R_{\hat{n}\hat{n}} = \mathbb{E}[\hat{n}\hat{n}^H] = (1-\rho)^2\, I_{N_r} \tag{24}$$

$$R_{\hat{e}\hat{e}} = \rho(1-\rho)diag(\mathbb{E}[yy^H]) \tag{25}$$

$$\begin{gathered} \mathbb{E}[yy^H] = (1-\zeta)^2 \frac{P_t}{N_S}\, HA_{RF}D_{BB}H^H {A_{RF}}^H {D_{BB}}^H \\ + \frac{\zeta(1-\zeta)}{N_S}\, P_t HA_{RF}diag(D_{BB}{D_{BB}}^H){A_{RF}}^H H^H \end{gathered} \tag{26}$$

Therefore,

$$\begin{gathered} R_{\hat{e}\hat{e}} = \rho(1-\rho)diag\left(\begin{matrix} k(1-\zeta)^2\frac{P_t}{N_S}HH^H \\ +k\zeta(1-\zeta)\frac{P_t}{N_S}HH^H + I_{N_r} \end{matrix}\right), \\ k = A_{RF}diag\left(D_{BB}{D_{BB}}^H\right){A_{RF}}^H \end{gathered} \tag{27}$$

Finally, by Eqs. (18), (22), (24), and (27) we get,

$$\begin{gathered} SE = log_2 \left| I_{N_r \times k} + \right. \\ \left. \zeta\frac{P_t}{N_S}(R_n)^{-1}HA_{RF}D_{BB}{D_{BB}}^H {A_{RF}}^H H^H \right| \end{gathered} \tag{28}$$

B. Precoder Design

1) Fully digital precoder design

The illustration of the Massive MIMO system with a Fully Digital Precoder is provided in Fig. 1, where each transmitter antenna is connected to a separate RF chain. The design of the Fully Digital Precoder is based on the NR CSI codebook approach, which involves using two matrices, W_1 and W_2, to construct the fully digital precoder D_{BB}. The W_2 matrix is created by taking the Kronecker Product of X_1 and X_2, where X_1 and X_2 are determined from the horizontal and vertical vectors of the antenna array (N_1 and N_2) and the DFT Oversampling vectors (O_1 and O_2) specified in the CSI codebook.

The CSI codebook provides a set of precoding matrices that can be used to design an FDP in a Massive MIMO system, depending on the number of antenna ports, antenna port configurations, and channel states. To use these precoding matrices, the transmitter sends different signals using different precoding matrices from the codebook. The receiver measures the quality of each signal (using, SINR) and decides which precoding matrix provided the best result. The receiver then feeds back the index of the best precoding matrix to the transmitter. The transmitter uses the chosen precoding matrix for future transmissions.

The resulting modified precoding matrix is then used to precode the data symbols at the transmitter before transmitting them to the UE. At the UE, the received signal is processed using the channel state information to decode the data symbols correctly. The values of the horizontal and vertical vectors (N_1 and N_2) and DFT oversampling vectors (O_1 and O_2) used in the construction of the W_2 matrix in the Fully Digital Precoder of the Massive MIMO system are specified in this codebook.

Although the Fully Digital Precoder is effective in achieving high SE, it may fall short in terms of power optimization because each antenna is connected to an individual RF chain. As a result, an optimal precoder design is necessary that can provide high SE performance while optimizing the EE as well. This requirement in Massive MIMO has resulted in the growing popularity of Hybrid Precoder Design, which can optimize both SE and EE.

Algorithm 1. Fully Digital Precoder Design

1	**Input**	$H, N_t{}^{RF}, N_S, CSI\ Codebook \leftarrow N_1, N_2, O_1, O_2, l, m$
2	**Output**	$Digital\ Precoder\ Matrix\ D_{BB}$
3	**Initially**	$[:,:,v] = SVD(H)$
4	**Then**	$V = inv(v) = W_1$
5	**Calculate**	$W_2 = X_1 \otimes X_2$
6		$X_1 = v_l = \left[1, e^{j\frac{2\pi l}{N_1 O_1}}, \dots, e^{j\frac{2\pi(N_1-1)l}{N_1 O_1}}\right]^T$,$X_2 = v_m = \left[1, e^{j\frac{2\pi m}{N_2 O_2}}, \dots, e^{j\frac{2\pi(N_1-1)m}{N_2 O_2}}\right]^T$
7	**Calculate**	$D_{BB} = W_1 \times W_2$

2) Hybrid precoder design

In this section, the focus is on designing a hybrid precoder to maximize the SE of the massive MIMO system. The iterative alternating minimization algorithm is used for this purpose and is presented in Algorithm 2. The algorithm starts with obtaining the Singular Value Decomposition (SVD) of the channel matrix H to obtain the optimal hybrid Precoded matrix W_{opt}.

The first step in the algorithm is to generate the analog Precoded matrix $\hat{A}$ using the expression $\hat{A} = e^{\angle[rand(N_t,N_r)}$, where N_t and N_r are the numbers of transmitter and receiver antennas, respectively. Then, by fixing this analog precoded matrix, the digital precoder matrix $\hat{D}$ is obtained. After obtaining the digital precoder matrix, it is fixed to obtain the optimal analog precoder matrix. This is done using the expression $A_{RF} = e^{\angle|F|}$, where $F = W_{opt}(\hat{D})^H$, and |F| represents the magnitude of the elements of F. The algorithm then checks if the SE has converged to a certain value, and if not, it updates the analog precoded matrix $\hat{A}$ and repeats the process until convergence is achieved. The final hybrid precoder matrix obtained in this way maximizes the SE of the massive MIMO system.

Algorithm 2. Iterative Alternating Minimization Algorithm for Precoder Design [18]

1	**Input**	$H, N_{RF}, N_S, Number\ of\ Iterations\ (i)$
3	**Output**	$Analog\ Precoder\ Matrix\ A_{RF}$ $and\ Digital\ Precoder\ Matrix\ D_{BB}$
4	**Initially**	$[:,:,v^H] = SVD(H), (v^H)' = W_{opt}$
5	**Then**	Calculate $\hat{A} = e^{\angle[rand(N_t,N_r)}$ with random phases
6	**for**	$1 \le i \le I\ do$
7		$Fix\ \hat{A}, calculate\ \hat{D} = (\hat{A})^H W_{opt}$
8		$calculate: F = W_{opt}(\hat{D})^H$
9		$fix\ \hat{D}, update\ \hat{A}, \hat{A} = e^{\angle|F|}$ end for
10		$A_{RF} = \hat{A},\ D_{BB} = \sqrt{N_S}\frac{\hat{D}}{\|A\hat{D}\|_F}$

$\hat{D}$ would be an optimal solution if the Power constraint is neglected. Therefore, by considering the transmit power constraint the optimal Digital Precoder Matrix D_{BB} is obtained by Equation represented in step 10 of Algorithm 2.

C. Analysis of Energy Efficiency

In this section we compute the EE of the system employing ADC and DAC with low resolution. Power consumed by each component of a considered communication system are listed in Table 2. Since EE is proportional to the SE, the EE is given [23]:

$$EE = \frac{B \times SE}{P_{tot}} \tag{29}$$

where B the Bandwidth of the system.

$$P_{tot} = P_{LO} + P_{PA} + 2N_r P_{ADC} + N_{RF}N_t P_{ps} + N_{RF}(2P_{DAC} + P_{RF}) \tag{30}$$

$$P_{RF} = 2P_M + 2P_{LF} + P_{HB}, P_{DAC} = c_1 f_1 q + c_2 2^q \text{ and } P_{ADC} = j f_r 2^b \tag{31}$$

Table 2. Power consumption by each device [18]

Device	Notation	Values
Local Oscillator	P_{LO}	22.5mW
Hybrid with buffer	P_{HB}	3mW
Power Amplifier	P_{PA}	P/0.25
Low Pass Filter	P_{LF}	14mW
Mixer	P_M	0.3mW
Phase Shifter	P_{PS}	21.6mW
RF Chain	P_{RF}	Eq. (31)
DAC	P_{DAC}	
ADC	P_{ADC}	

where c_1 is a coefficient of Static Power Consumption $= 9 \times 10^{-12}$, c_2 is Dynamic Power Consumption $= 1.5 \times 10^{-5}$ [23], f_t is the sampling rate at transmitter, f_r is the sampling rate at receiver, and j is the consumption of energy per conversion step.

VI. Simulation Results

In this section, we provide the obtained simulation results of a proposed precoded Massive MIMO System in which Low-resolution ADC/DACs are considered and undergo UQ and NUQ processes. In the proposed work Point-to-Point Massive MIMO system is considered with Base Station equipped with N_t transmitter Antennas, $N_{RF}{}^t$ RF chains, and $\boldsymbol{q}$ Resolution DACs whereas Receiver is equipped with N_r Number of receiver antennas, $N_{RF}{}^r$ RF chains, and $\boldsymbol{b}$ Resolution ADCs. The number of data streams is considered as N_S. A narrow-band Rayleigh-fading channel with perfect synchronization and with no inter-symbol interference is assumed [18]. The simulation results obtained are averaged over multiple iterations.

Initially, we examine the SE of a Fully Digital Precoder in a Base Station equipped with N_t transmitter antennas, with each antenna linked to an individual RF Chain, as depicted in Fig. 1. In this scenario, both the DAC and ADC resolutions are considered to be infinite. Next, we evaluate the performance of a Hybrid Precoded Point-to-Point Massive

MIMO system using UQ and NUQ. This analysis involves investigating the impact of finite resolution ADC with varying DAC resolutions of 2,4, and 6 bits, as well as finite resolution DAC with varying ADC resolutions of 2,4, and 6 bits. In Fig. 3, we assess the performance of a Single User Point to Point Massive MIMO System with Full Digital Precoding (Algorithm 1), where $N_t = 64$, $N_r = 36$, $N_s = 2$ and ${N_{RF}}^t = 2$, $q = \infty, b = \infty$.

As seen in Fig. 3, the SE for both UQ and NUQ is identical, with an SNR above $-10dB$. With an increase in the resolution of ADC and DAC, we can observe an improvement and an increase in SE with increasing SNR. Another crucial factor is that each transmitter antenna is linked to an individual RF chain. Thus, increasing the number of antennas at the Base Station results in a more optimal SE. For both UQ and NUQ, Fig. 4 illustrates the performance evaluation of a Massive MIMO system using a hybrid precoder with varied DAC resolutions ($q = 2,4,6\ bits$).

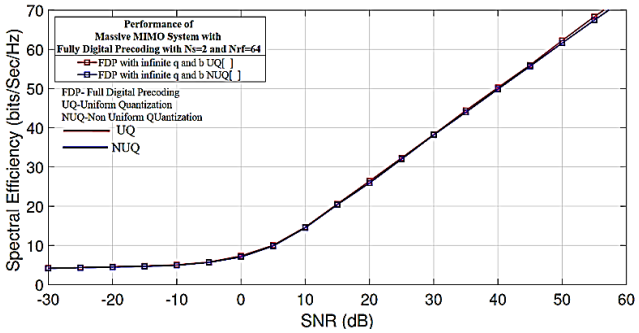

Fig. 3. SE with $q =$ High Resolution and $b =$ High Resolution . $N_t = 64$, $N_r = 36$, $N_s = 2$ and ${N_{RF}}^t = 2$.

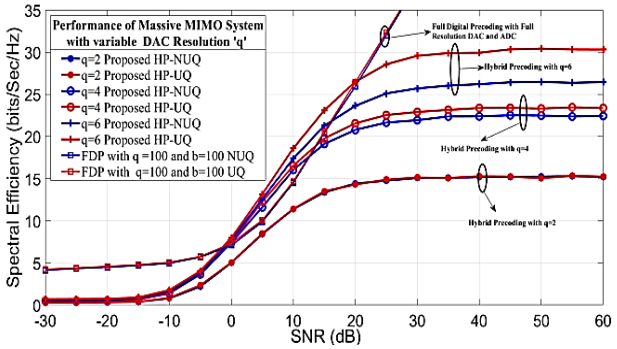

Fig. 4. SE with varying q and fixed High Resolution b. $N_t = 64$, $N_r = 36$, $N_s = 2$ and ${N_{RF}}^t = 2$.

The Alternating Minimization Precoding Algorithm (Algorithm 2) is used to create the suggested hybrid precoder for both UQ and NUQ instances. According to the simulation results, NUQ uses fewer quantization bits than UQ to attain almost the same SE at $SNR > 0dB$. Due to the Gaussian white noise power being near to the transmitted power at low SNRs ($-30dB > SNR > -10dB$), the spectral efficiency of both UQ and NUQ is almost the same for varied DAC resolutions. As SNR rises, the SE rises as well ($from\ 0dB$). The SE with different DAC resolutions is higher at high SNRs ($> 20dB$). The achieved SE in both the UQ and NUQ situations is practically identical to the fully digital precoder's performance at a specific SNR, as shown in Table 3, demonstrating how close the proposed system's performance is to FDP. Moreover, SE rises in tandem with the DAC resolution.

Table 3. Values of SE (Bits/Sec/Hz) of massive MIMO system with varied $'q'$ and fixed high resolution $'b'$

Type of a System	Varying DAC Resolution		
	q = 2	q = 4	q = 6
FDP with UQ	18.27	26.75	34.27
FDP with NUQ	18.27	23.2	26.86
HP with UQ	16.26	27.4	31.6
HP with NUQ	16.26	24.05	25.34

With the system parameters set to $N_t = 64$, $N_r = 36$, $N_s = 2$, and ${N_{RF}}^t = 2$ in Fig. 5, the performance of the same system is assessed by altering ADC resolution and SNR. The suggested Hybrid Precoder is assessed in both UQ and NUQ situations and was created utilizing the Alternating Minimization Precoding Algorithm. According to the simulation results, raising the ADC resolution can enhance SE performance to a level where it is similar to the system without quantization distortion. Table 4 displays the SE values from the simulation at a given SNR. It can be shown that, in both the UQ and NUQ situations, the proposed work's SE is nearly identical to the Fully Digital Precoder performance.

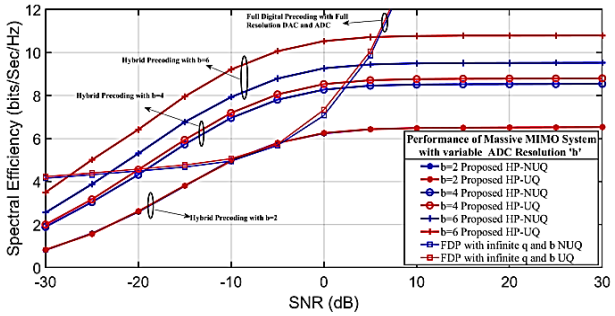

Fig. 5. SE with varying b and Fixed High Resolution q. $N_t = 64$, $N_r = 36$, $N_s = 2$ and ${N_{RF}}^t = 2$

TABLE 4. Values of SE of massive MIMO system with varied $'\boldsymbol{b}'$ and fixed $'\boldsymbol{q}'$

Type of a System	Varying ADC Resolution		
	b = 2	b = 4	b = 6
FDP with UQ	4.356	4.787	4.982
FDP with NUQ	4.356	4.679	4.871
HP with UQ	4.685	5.058	5.129
HP with NUQ	4.685	5.058	5.058

Figs. 6 and 7 illustrate the EE of the Massive MIMO system as a function of varying q and b at a particular Signal-to-Noise Ratio (SNR) of 5 dB. Notably, similar EE performance is observed in both UQ and NUQ cases when varying q, whereas UQ outperforms NUQ when varying b.

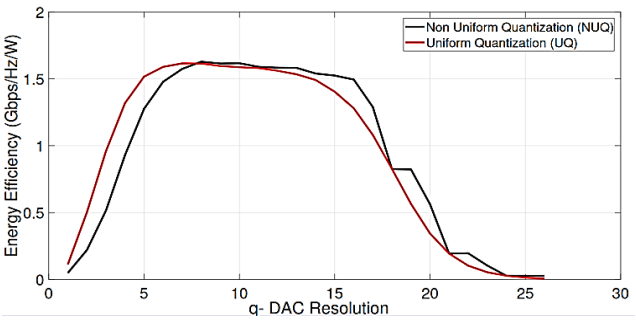

Fig. 6. EE vs q with $b = 6$.

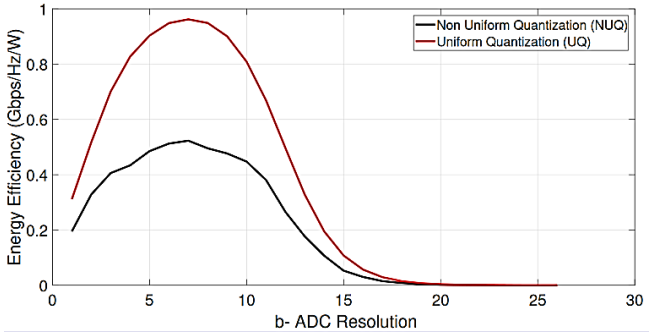

Fig. 7. EE vs b with $q = 6$.

Fig. 8 depicts the EE vs SE variation for different q, with an SNR of 5 dB and ADC resolution $b = 6$, in the HP scenario. Fig. 9 presents the same variation for the FDP case. It can be observed that the curves increase linearly until they reach maximum EE and then start declining in Fig. 8. This occurs because the number of bits that can be transmitted after an SNR threshold increases incrementally with a significant rise in power. Comparing Fig. 8 to Fig. 9, it is evident that the proposed work's SE is nearly equivalent to FDP, while EE is significantly optimized in the proposed work, as compared to FDP, as seen in Table 5.

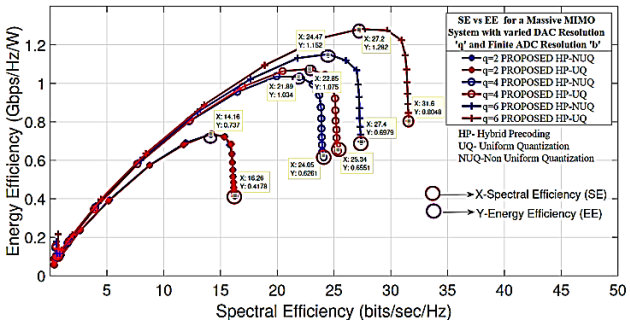

Fig. 8. Proposed: EE vs. SE comparison for varied DAC q with ADC $b = 6$.

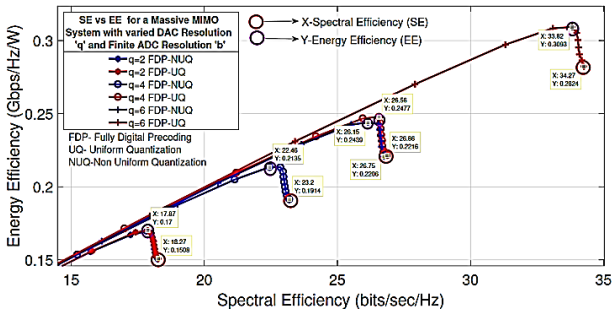

Fig. 9. FDP: EE vs. SE comparison for varied DAC q with ADC $b = 6$.

Table 5. The EE of massive MIMO system with varied $'q'$ and fixed $'b = 6\ bits'$

Type of a System	Varying DAC Resolution		
	$q = 2$	$q = 4$	$q = 6$
FDP with UQ	0.17	0.2439	0.3093
FDP with NUQ	0.17	0.2135	0.2477
HP with UQ	0.737	1.152	1.282
HP with NUQ	0.737	1.034	1.075

Similarly, we can see in Fig. 10 which shows the variation of EE vs SE for varying b case at an SNR of 5 dB and $q = 6$. Fig. 11 shows the variation of EE vs SE for varying b case at an SNR of 5 dB for the FDP case and $q = 6$ is considered. The performance is similar to the earlier case which can be seen in Table 6 in which the proposed work SE is approximately equal to FDP whereas EE is much optimized in the proposed work as compared to FDP.

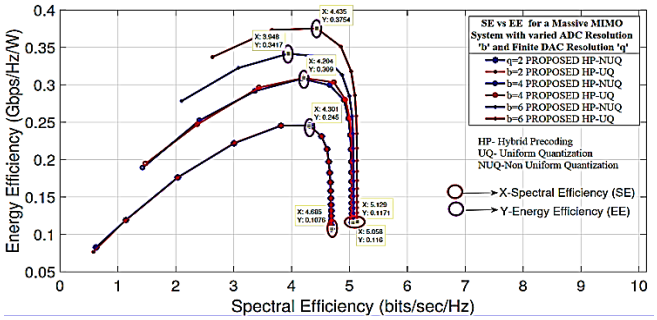

Fig. 10. Proposed: EE vs. SE comparison for varied ADC b with DAC $q = 6$.

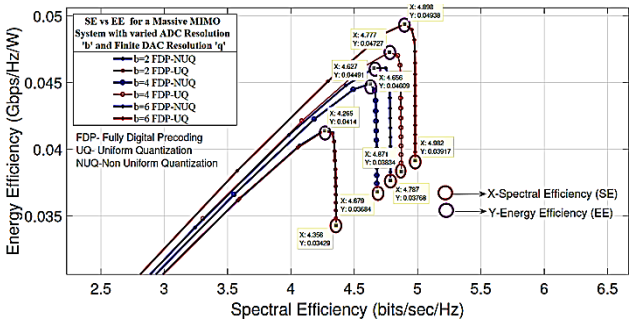

Fig. 11. FDP: EE vs. SE comparison for varied ADC b with DAC $q = 6$.

Table 6. The EE of massive MIMO system with varied $'\boldsymbol{b}'$ and fixed $'q = 6\ bits'$

Type of a System	Varying ADC Resolution		
	$b = 2$	$b = 4$	$b = 6$
FDP with UQ	0.0414	0.0465	0.0493
FDP with NUQ	0.0414	0.0449	0.0472
HP with UQ	0.245	0.3417	0.3754
HP with NUQ	0.245	0.309	0.309

Further, from the graph, it can be observed that, for $q = 2$, both UQ and NUQ have similar trade-off curves, this is because in both cases the quantizer resolution is 2 bits. For $q = 4$ the gap between NUQ and UQ is wider when compared with that of $q = 2$ and for $q = 6$ the gap between NUQ and UQ is much wider when compared with that of $q = 4$. At lower SNRs, for the same SE, NUQ achieves more EE than UQ. This is because; NUQ needs less amount of DAC resolution when compared with that of UQ.

VII. Conclusion and Future Work

In this paper, we conducted a comprehensive study on HP in single-user point-to-point massive MIMO systems with low-resolution ADCs and DACs. Through a thorough literature review and simulation analysis, we investigated the impact of UQ and NUQ techniques on system performance. Our results demonstrated that both UQ and NUQ can achieve high SE in the considered system. However, NUQ showed superior performance in terms of EE by allocating more bits to perceptually important signal components. Furthermore, we compared the FDP with the hybrid precoder design and observed that the hybrid precoder achieved comparable SE performance to the FDP while offering improved EE. Overall, our findings highlight the significance of NUQ techniques and the advantages of HP for achieving a balance between SE and EE in massive MIMO systems with low-resolution ADCs and DACs.

In the future, we plan to explore the integration of machine learning algorithms to further optimize HP in the context of massive MIMO systems with low-resolution ADCs and DACs. Specifically, we aim to investigate the application of reinforcement learning techniques to adaptively optimize precoding policies based on real-time channel conditions and system constraints. Additionally, we will explore the use of deep learning algorithms for more accurate channel estimation and prediction, which can enhance the performance of HP systems. Another area of interest for future research is the exploration of different non-uniform quantization schemes and their impact on system performance. We will consider joint optimization of quantization and precoding using machine learning approaches to achieve even higher SE and EE. The integration of machine learning algorithms in optimizing HP presents promising opportunities to enhance system performance, adapt to varying channel conditions, and improve overall efficiency in massive MIMO systems.

In summary, this study contributes to the understanding of HP in massive MIMO systems with low-resolution ADCs and DACs. Our findings emphasize the importance of non-uniform quantization techniques and highlight the advantages of HP for achieving a balance between SE and EE. The future work outlined here, involving the integration of machine learning algorithms, offers exciting prospects to further optimize HP and enhance the performance of massive MIMO systems in practical scenarios. By combining advanced signal processing techniques with machine learning, we can unlock the full potential of massive MIMO technology and pave the way for efficient and high-performing wireless communication systems.

CONFLICT OF INTEREST

The authors declare no conflict of interest.

AUTHOR CONTRIBUTIONS

Girish Kumar N G conceived the idea, designed the analysis for the Hybrid Precoder Design using a Non-Uniform Quantization algorithm for Low-resolution ADCs and DACs, and performed the data analysis. Dr. M N Sree Ranga Raju provided supervision and guidance throughout the project. Both authors participated in interpreting the results and drawing the conclusions presented in this work. Girish Kumar N G drafted the manuscript, and Dr. M N Sree Ranga Raju made substantial revisions. All authors read and approved the final version of the manuscript.

ACKNOWLEDGMENT

I would like to thank Dr. Sadashivappa G, BOE, RVCE, Bangalore, and Dr. Ivan Jose, Academic Dean, Christ University for their valuable support and guidance throughout this work.

REFERENCES

[1] R. Chataut and R. Akl, "Massive MIMO systems for 5G and beyond networks—Overview, recent trends, challenges, and future research direction," *Sensors*, vol. 20, no. 10, 2753, 2020.

[2] W. Hong *et al*., "The role of millimeter-wave technologies in 5G/6G wireless communications," *IEEE Journal of Microwaves*, vol. 1, no. 1, pp. 101–122, Jan. 2021. doi: 10.1109/JMW.2020.3035541

[3] J. Zhang, X. Yu, and K. B. Letaief, "Hybrid beamforming for 5G and beyond millimeter-wave systems: A holistic view," *IEEE Open Journal of the Communications Society*, vol. 1, pp. 77–91, 2020. doi: 10.1109/OJCOMS.2019.2959595

[4] Y. Hei, S. Yu, C. Liu, W. Li, and J. Yang, "Energy-efficient hybrid precoding for mmWave MIMO systems with phase modulation array," *IEEE Transactions on Green Communications and Networking*, vol. 4, no. 3, pp. 678–688, Sept. 2020. doi: 10.1109/TGCN.2020.2974282

[5] C. Chen, Y. Wang, S. Aïssa, and M. Xia, "Low-complexity hybrid analog and digital precoding for mmWave MIMO systems," in *Proc. 2020 IEEE 31st Annual International Symposium on Personal, Indoor and Mobile Radio Communications*, 2020, pp. 1–6. doi: 10.1109/PIMRC48278.2020.9217058

[6] Q. Ding, Y. Deng, X. Gao, and M. Liu, "Hybrid precoding for mmWave massive MIMO systems with different antenna arrays," *China Communications*, vol. 16, no. 10, pp. 45–55, Oct. 2019. doi: 10.23919/JCC.2019.10.003

[7] A. Salh, L. Audah, N. S. M. Shah *et al*., "Energy-efficient power allocation with hybrid beamforming for millimeter-wave 5G massive MIMO system," *Wireless Pers. Commun.*, vol. 115, pp. 43–59, 2020. https://doi.org/10.1007/s11277-020-07559-w

[8] A. A. Salem, S. El-Rabaie, and M. A. Shokair, "Proposed efficient hybrid precoding algorithm for millimeter wave massive MIMO 5G networks," *Wireless Pers. Commun.*, vol. 112, pp. 149–167, 2020. https://doi.org/10.1007/s11277-019-07020-7

[9] J. P. Pavia, V. Velez, R. Ferreira, N. Souto, M. Ribeiro, J. Silva, and R. Dinis, "Low complexity hybrid precoding designs for multiuser mmWave/THz ultra massive MIMO systems," *Sensors*, vol. 21, no. 18, 6054, 2021. https://doi.org/10.3390/s21186054

[10] Z. Lu, Y. Zhang, and J. Zhang, "Quantized hybrid precoding design for millimeter-wave large-scale MIMO systems," *China Communications*, vol. 16, no. 4, pp. 130–138, April 2019. doi: 10.12676/j.cc.2019.04.010

[11] T. Li and F. Zhao, "A spectral efficient hybrid precoding algorithm for mmWave MIMO systems," *Procedia Computer Science*, vol. 174, pp. 584–590, 2020. https://doi.org/10.1016/j.procs.2020.06.128

[12] T. Ren and Y. Li, "Hybrid precoding design for energy efficient millimeter-wave massive MIMO systems," *IEEE Communications Letters*, vol. 24, no. 3, pp. 648–652, March 2020. doi: 10.1109/LCOMM.2019.2960249

[13] A. W. Shaban, O. Damen, Y. Xin, and E. Au, "Statistically-aided codebook-based hybrid precoding for millimeter wave channels," *IEEE Access*, vol. 8, pp. 101500–101513, 2020. doi: 10.1109/ACCESS.2020.2997190

[14] Y. Huang, C. Liu, Y. Song *et al*., "DFT codebook-based Hybrid Precoding for multiuser mmWave massive MIMO systems," *EURASIP J. Adv. Signal Process*, 11, 2020. https://doi.org/10.1186/s13634-020-00669-4

[15] A. Almradi, M. Matthaiou, P. Xiao, and V. F. Fusco, "Hybrid precoding for massive MIMO with low-rank channels: A two-stage user scheduling approach" *IEEE Transactions on Communications*, vol. 68, no. 8, pp. 4816–4831, Aug. 2020. doi: 10.1109/TCOMM.2020.2991805

[16] W. Zhang, X. Xia, Y. Fu, and X. Bao, "Hybrid and full-digital beamforming in mmWave Massive MIMO systems: A comparison considering low-resolution ADCs," *China Communications*, vol. 16, no. 6, pp. 91–102, June 2019. doi: 10.23919/JCC.2019.06.008

[17] J. Liu, J. Dai, J. Wang *et al.*, "Achievable rates for full-duplex massive MIMO systems with low-resolution ADCs/DACs under imperfect CSI environment," *J. Wireless Com. Network*, 222, 2018.

[18] J. Dai, J. Liu, J. Wang, J. Zhao, C. Cheng, and J.-Y. Wang, "Achievable rates for full-duplex Massive MIMO systems with low-resolution ADCs/DACs," *IEEE Access*, vol. 7, pp. 24343–24353, 2019. doi: 10.1109/ACCESS.2019.2900273

[19] Q. Ding, Y. Deng, and X. Gao, "Spectral and energy efficiency of HP for mmWave massive MIMO with low-resolution ADCs/DACs," *IEEE Access*, vol. 7, pp. 186529–186537, 2019.

[20] Y. Xiong, "Achievable rates for massive MIMO relaying systems with variable-bit ADCs/DACs," *IEEE Communications Letters*, vol. 24, no. 5, pp. 991–994, May 2020. doi: 10.1109/LCOMM.2020.2971467

[21] Q. Ding, Y. Lian, and Y. Jing, "Performance analysis of full-duplex massive MIMO systems with low-resolution ADCs/DACs over Rician fading channels," *IEEE Transactions on Vehicular Technology*, vol. 69, no. 7, pp. 7389–7403, July 2020. doi: 10.1109/TVT.2020.2991143

[22] Q. Xu and P. Ren, "Secure massive MIMO downlink with low-resolution ADCs/DACs in the presence of active eavesdropping," *IEEE Access*, vol. 8, pp. 140981–140997, 2020. doi: 10.1109/ACCESS.2020.3013635

[23] Y. Xiong, S. Sun, N. Wei, L. Liu, and Z. Zhang, "Performance analysis of massive MIMO relay systems with variable-resolution ADCs/DACs over spatially correlated channels," *IEEE Transactions on Vehicular*

Technology, vol. 70, no. 3, pp. 2619–2634, March 2021. doi: 10.1109/TVT.2021.3061699

[24] H. Wang, C. Sun, J. Li *et al.*, "Joint optimization of spectral efficiency and energy efficiency with low-precision ADCs in cell-free massive MIMO systems," *Sci. China Inf. Sci.*, vol. 65, 152301, 2022. https://doi.org/10.1007/s11432-021-3313-9

[25] X. Zhang, T. Liang, K. An, G. Zheng, and S. Chatzinotas, "Secure transmission in cell-free massive MIMO with RF impairments and low-resolution ADCs/DACs," *IEEE Transactions on Vehicular Technology*, vol. 70, no. 9, pp. 8937–8949, Sept. 2021. doi: 10.1109/TVT.2021.3098693

[26] J. Li, A. Wan, M. Zhou, J. Yuan, R. Yin, and L. Yang, "Downlink analysis for the D2D underlaid multigroup multicast cell-free massive MIMO with low-resolution ADCs/DACs" *IEEE Access*, vol. 10, pp. 115702–115715, 2022. doi: 10.1109/ACCESS.2022.3218721

[27] Y. Zhang, D. Li, D. Qiao, and L. Zhang, "Analysis of indoor THz communication systems with finite-bit DACs and ADCs," *IEEE Transactions on Vehicular Technology*, vol. 71, no. 1, pp. 375–390, Jan. 2022. doi: 10.1109/TVT.2021.3123380

[28] E. Balti and B. L. Evans, "Full-duplex massive MIMO cellular networks with low resolution ADC/DAC," in *Proc. 2022 IEEE Global Communications Conference*, 2022, pp. 1649–1654. doi: 10.1109/GLOBECOM48099.2022.10001148

[29] M. Zhou, Y. Zhang, X. Qiao, M. Xie, L. Yang, and H. Zhu, "Multigroup multicast downlink cell-free massive MIMO systems with multiantenna users and low-resolution ADCs/DACs," *IEEE Systems Journal*, vol. 16, no. 3, pp. 3578–3589, Sept. 2022. doi: 10.1109/JSYST.2021.3077765

[30] I.-S. Kim, M. Bennis, and J. Choi, "Cell-free mmWave massive MIMO systems with low-capacity fronthaul links and low-resolution ADC/DACs," *IEEE Transactions on Vehicular Technology*, vol. 71, no. 10, pp. 10512–10526, Oct. 2022. doi: 10.1109/TVT.2022.3184172

[31] W. Zhang, J. Xia, and X. Bao, "Massive MIMO systems with low-resolution ADCs: Achievable rates and allocation of quantization bits," *Wireless Communications and Mobile Computing*, vol. 2023, 4012841, 2023. https://doi.org/10.1155/2023/4012841

[32] J. Park, N. Lee, S. Hong, and Y. Jeon, "Learning from noisy labels for MIMO detection with one-bit ADCs," *IEEE Wireless Communications Letters*, vol. 12, pp. 456–460, Mar. 2023.

[33] L. Wen, H. Qian, Y. Hu, Z. Deng, and X. Luo, "One-bit downlink precoding for massive MIMO OFDM system," *IEEE Transactions on Wireless Communications*, January 2023.